Sixth International Symposium on Marine Propulsors
smp'19, Rome, Italy, May 2019

A Study on Deformation Measurements and Hydrodynamic Investigation of the Flexible Composite Marine Propeller

Koichiro Shiraishi[1], Yuki Sawada[1], Daijiro Arakawa[1], Koyu Kimura[2]

[1]National Maritime Research Institute (NMRI), Tokyo, Japan
[2]Akishima Laboratories (Mitsui Zosen) Inc., Tokyo, Japan

ABSTRACT

In this paper, authors have developed an estimation method for deformed blade shape of flexible composite marine propellers. The authors have recently developed a 3D shape measurement system using Combination line CCD camera method and confirmed that the system can measure deformation of a model propeller with enough accuracy. However, in order to utilize the results of the deformation measurement as verification data for fluid structure interaction calculation, not only the amount of deformation, but the deformed 3D blade shape is necessary.

The authors focus on a feature that the deformed blade shape can be represented by the position change of the wing section and developed an estimation method for the deformed blade shape by image-registration. For verification of the system's effectiveness, model experiments were conducted in the NMRI's large cavitation tunnel using the highly skewed propeller of a training ship "Seiun-Maru-I". Comparing the results of experiments and numerical simulation, the authors show the effectiveness of the developed estimation method.

Keywords

Flexible composite marine propeller, Deformation measurements, Combination line CCD camera method, Hydrodynamic characteristics and image-registration.

1 INTRODUCTION

In order to improve theoretical prediction of deformation and propeller characteristics of CFRP propeller, it is indispensable to investigate the behavior of deformation of the propeller blades. Authors have already developed a 3D shape measurement system using the combination line CCD camera method and confirmed that the system can measure the deformation of a model propeller with enough accuracy (Hoshino 2014, Kawakita 2016). However, in order to utilize the measurement results of the deformation as verification data for fluid structure interaction calculation, not only the amount of deformation, but the deformed 3D blade shape is necessary (Taketani 2013). Therefore, the authors focus on a feature that the deformed blade shape can be represented by the position change of the wing section of the propeller. An estimation method for deformed blade shape of flexible composite marine propellers using image-registration have been developed. The image-registration is a pose estimation method used in the field of computer vision. To verify effectiveness of the developed estimation method, model experiments using a highly skewed propeller-of a training ship "SEIUN-MARU I" has been carried out in the large cavitation tunnel of NMRI (Kurobe 1983). The deformed propeller's characteristics is estimated by numerical calculation. The authors show the deformed shape estimation are effective for investigation of the influence of propeller deformation on fluid performance.

2 DEFORMATION MEASUREMENT

2.1 Combination-line CCD camera measurement method

The combination of line CCD cameras have been used for measuring of cavity shapes on the model propeller (Shiraishi et al 2004). In this method, a laser beam is irradiated onto a measurement object and light scattered from its surface is photographed using three-line CCD cameras. Based on the resulting image data, the three-dimensional surface of the object is reconstructed via triangulation.

In line CCD cameras, the image-receiving elements are arranged in a row. Such cameras have the advantage of much higher scan rates and resolution than area CCD cameras. The configuration and a photo of the camera system used in this study for three-dimensional shape measuring are shown in Figures 1. The authors used a green laser (532 nm), a wavelength with high penetration ability in water.

---

[*] Leave blank the last 2.0 cm on the first page to place some additional informational about this paper in a footnote on the first page if necessary.

The specific measurement method used by the proposed system is outlined as follows. Firstly, the laser beam is used to irradiate the position to be measured, with laser light scattered from the surface of the measurement object passed through a semi-cylindrical lens and focused onto the line CCD elements for imaging. Triangulation is then used to extract the three-dimensional coordinates of the laser light spot position from the peak coordinates of the luminance distributions of the images captured by the cameras. Figure 3 shows the measurement principle applied by the combined-line CCD method as seen from the depth direction.

Figure 1 Photo of 3D shape measurement system.

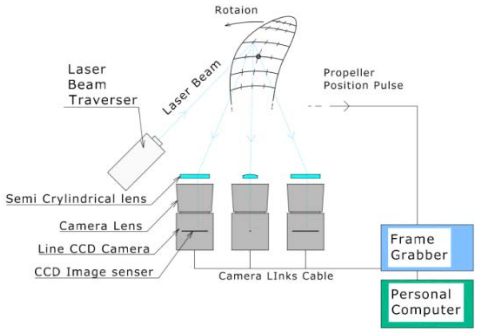

Figure 2 Schematic of measurement system

In the figure 3, $P(X_0, Y_0, Z_0)$ is the measurement point and A and B are the installation positions of the left- and right-line CCD cameras, respectively. Using the principle of triangulation, the three-dimensional coordinates of the laser spot light can be calculated from the following equations:

$$X_0 = d \cdot X_L/(X_L - X_R) = X_L \cdot Z_0/f \quad (1)$$

$$Y_0 = d \cdot X_C/(X_L - X_R) = Y_C \cdot Z_0/f \quad (2)$$

$$Z_0 = d \cdot f/(X_L - X_R) \quad (3)$$

where X_L, X_R, Y_C are the coordinates of the peak position of the laser on the captured image of each camera, $(X_L - X_R)$ is the parallax between the left and right cameras,d is the distance between points A and B, and f is the focal length of each camera.

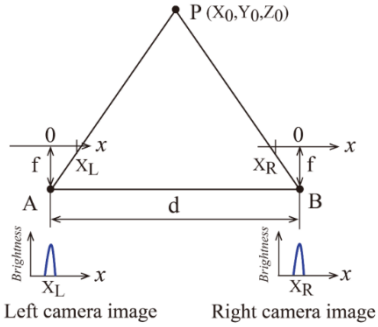

Figure 3 Illustration of the use of triangulation in the combination-line CCD camera method

2.2 Deformation measurement procedure

The deformation measurement is conducted by the following procedure using the combination line CCD method. The laser beam is irradiated to a white dot on a model propeller. The white dot is the measurement position. The scattered light is photographed by the three line CCD cameras. The peak position is detected from brightness distribution of obtained images. The three-dimensional position of the measurement point is calculated by the principle of triangulation on peak position. The amount of deformation is calculated by comparing the mark positions between the base condition and test conditions. Figure 4 shows a scenery of the defamation measurement in the cavitation tunnel at NMRI.

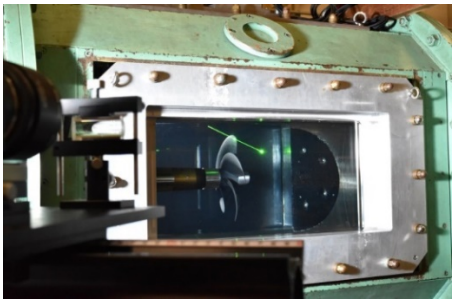

Figure 4 Photo of deformation measurements of model propeller.

2.3 Experiment setting

In this research, highly skewed propeller (HSP) of Seiun-Maru-I is selected to verify the present calculation. Figure 5 shows the model propeller of HSP used in the deformation measurement. The material of the model propeller is carbon filled nylon. The principal parameters and material properties of the propeller are provided in Table 1 and Table 2, respectively. One of the five propeller blades was painted with white dots which become a measurement point for the deformation.

Deformation measurements in the experiments were made using an O-XYZ spatial coordinate system (Figure 6). The shape of the propeller blades was measured at a propeller phase angle of 0° with a positive counterclockwise rotation

of 22.0 revolutions per second [rps]. Figure 8 shows the cavitation tunnel with the experimental system in place.

Figure 9 shows the layout of the system, with the three line CCD cameras and the green laser emitter located outside of the cavitation tunnel.

Figure 5 Photo of the model propeller.

Table. 1 Principal particulars of model propeller.

Diameter [m]	0.250
Pitch Ratio at 0,7R	0.944
Expanded Area Ratio	0.700
Boss Ratio	0.1972
Number of Blade	5
Skew Angle [deg.]	45.0

Table. 2 Material properties of model propeller.

Maximum tensile stress [MPa]	77.8
Tensile modulus of elasticity [MPa]	7320.0
Maximum bending stress [MPa]	131.5
Bending elastic modulus [MPa]	6248.0

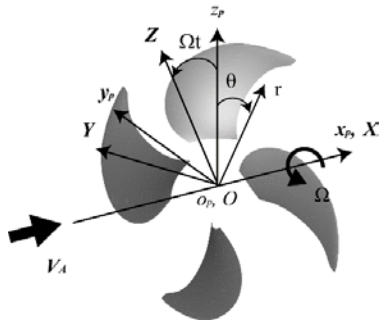

Figure 6 Coordinate systems of propeller.

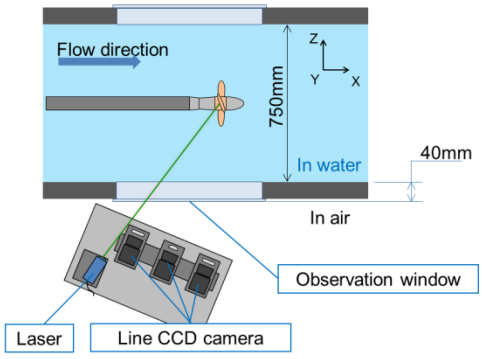

Figure 7 Top view of measurement system layout

2.4 Results of Deformation Measurement

In figure 8 and figure 9, the results of deformation measurement are shown. In both figures, black dots indicate white marker positions before deformation, and the red dots indicate white marker positions at propeller rotation speed 22.0 [rps]. However, the marker position before deformation is the value calculated from the propeller offset data. From these figures, it can be confirmed that the blade tip is bent in the back surface of the model propeller direction by the developed measurement system. Figure 10 show the measurement results position of the blade cross section at each radial position in the xy plane. From these figures, it is confirmed that although the blade cross section of 0.6R near the blade root hardly changes, the displacement increases as it approaches the blade tip. Fig. 13 shows the measurement position at the center of the cord length at each radial position at each rotation speed in the xz plane. This figure also confirms that the model propeller is bent in the back surface direction (-x direction).

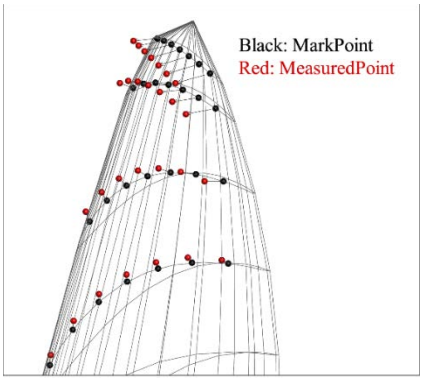

Figure 8 Results of propeller deformation measurement

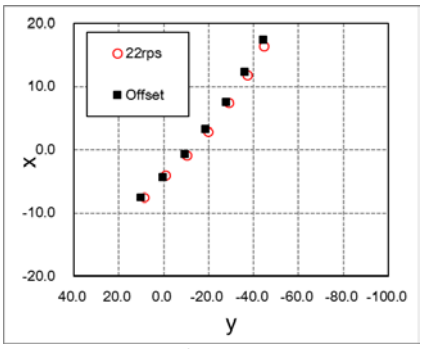

(1) Deformation at 0.7R

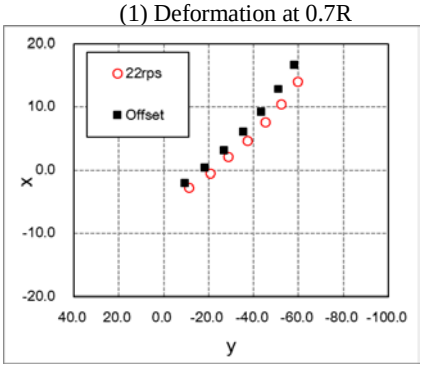

(2) Deformation at 0.8R

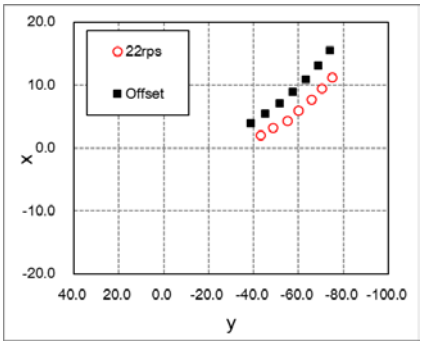

(3) Deformation at 0.9R

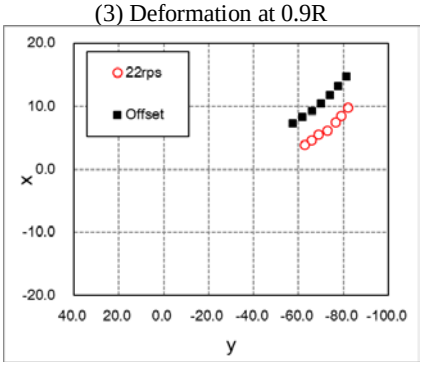

(4) Deformation at 0.95R

Figure 9 Comparison propeller surface original shapes and deformed shapes at x-y plane at 0.7R, 0.8R. 0.9R, 0.95R.

3 ESTIMATION METHOD FOR DEFORMED BLADE SHAPES

3.1 Image-registration

In this research, the authors have estimated the deformed blade shape using an image-registration (Arun 1987). The image-registration is a pose estimation method used in the field of computer vision. In the image-registration, it is assumed that the relative position and orientation of a set of points given correspondences are represented by a rotation matrix **R** and a translation vector **t**. Then, it is a method to determine the rotation matrix and translation vector so that the error between corresponding points of point sets is minimized. This problem is formulated as the following equation with the sum of squares of the distance between corresponding points as the minimization problem.

$$\min_{\boldsymbol{R},\boldsymbol{t}} \sum_{i=1}^{N} \|y_i - (\mathbf{R}x_i + \mathbf{t})\|^2 \qquad (4)$$

Here, N is the number of reference points, x_i is i th point of set X, y_i is i th point of set Y. The minimization problem represented by equation (4) can be solved by using singular value decomposition (SVD). The rotation matrix and the translation vector are obtained from the solution of equation (4).

3.2 Deformed Shape Estimation

The estimation of the deformed wing shape using the image-registration is performed as follows. First, image-registration is applied to marker positions before and after deformation, and rotation matrices and translation vectors are calculated for each blade cross section. Next, the position of each wing section after deformation is estimated using the calculated rotation matrix and translation vector. Finally, by connecting the wing sections, the three-dimensional wing shape after deformation is estimated. In figure 10, the illustration of deformed shape estimation using image-registration.

The result of estimating the deformed blade shape using the deformation measurement results shown in the previous section is shown in figure 11 and figure 12. From these figures, it can be confirmed from the deformation measurement results that the deformed blade shape can be estimated.

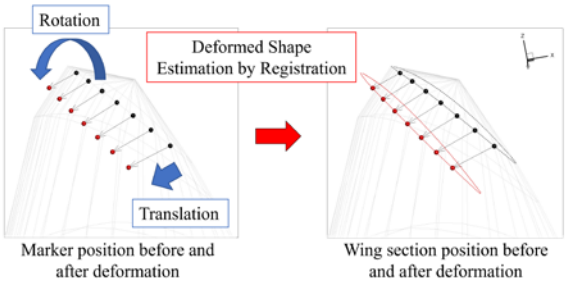

Figure 10 Illustration of deformed shape estimation using image-registration

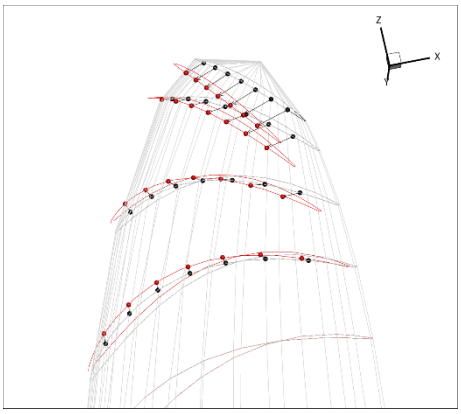

Figure 11 Estimated wing section positions of the model propeller.

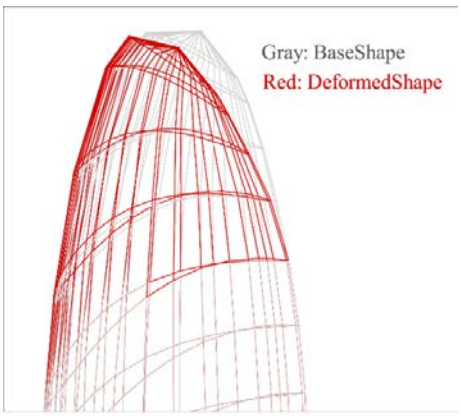

Figure 12 Estimated deformed shape of the model propeller.

4 NUMERICAL SIMULATION

4.1 QCM

In this study, QCM (Quasi-Continuous vortex lattice Method) was used to estimate propeller performance after deformation. QCM is a numerical method based on the lifting surface theory, which was developed by Lan (Lan 1974) originally to solve planar wing problems. Since its development, it has been successfully applied to estimation of the thrust and torque of various propellers in a uniform and non-uniform inflow (Shiraishi 2015, Hoshino 1985 and Nakamura 1985).

4.2 Results of Numerical Simulation

Propeller characteristics and pressure distribution of the post-deformation propeller estimated by image-registration were calculated using QCM. Figure 13 shows a comparison of the results of numerical simulation and experimental results for propeller characteristics. Blue bars indicate experimental results. red bars indicate results of the numerical simulations. The propeller thrust coefficient K_T , the propeller torque coefficient K_Q and propeller coefficient are defined using equation (5)-(7) wherein ρ [kg/m^3] is the water density, D_p [m] is the propeller diameter, n [rps] is propeller rotation number, T[N] is the thrust of propeller, Q[N·m] is the torque of propeller and J is the advanced coefficient.

$$K_T = \frac{T}{\rho n^2 D_p^4} \tag{5}$$

$$K_Q = \frac{Q}{\rho n^2 D_p^5} \tag{6}$$

$$\eta_o = \frac{JK_T}{2\pi KQ} \tag{7}$$

From this figure, it is found that the results of model experiment are in good agreement with and the numerical simulation. These results show that the deformed shape estimation method using registration is effective.

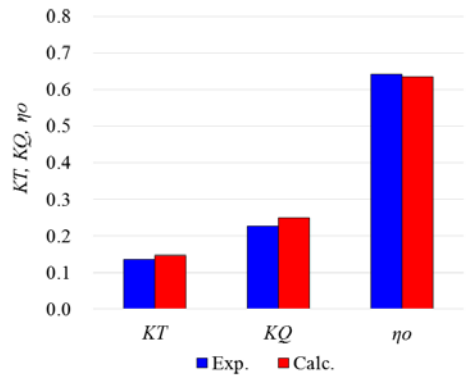

Figure 13 Comparison of propeller characteristics between experiments and estimations.

Figure 14 shows pressure distributions on propeller surfaces estimated by QCM. Blue lines show the pressure distribution of the propeller before deformation. Red lines show the pressure distribution of the propeller after deformation. From these figures, it is found that the difference pressures between face and back surface around the blade tip (0.95R, 0.9R and 0.8R) is smaller than the middle of the blade. This means that the blade tip is deformed to decrease the load on the blade. It is consistent with the result of the model experiment.

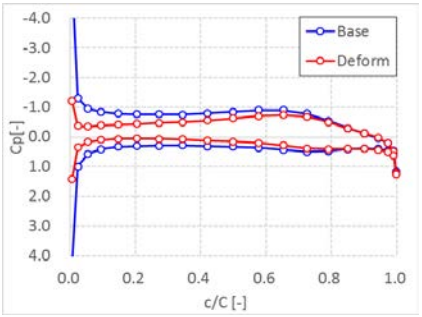

(1) Pressure distribution at 0.95R

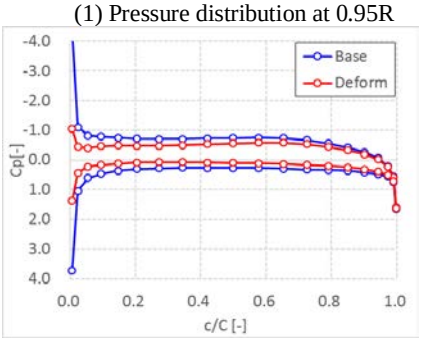

(2) Pressure distribution at 0.9R

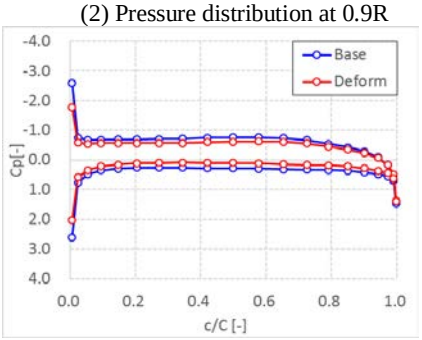

(3) Pressure distribution at 0.8R

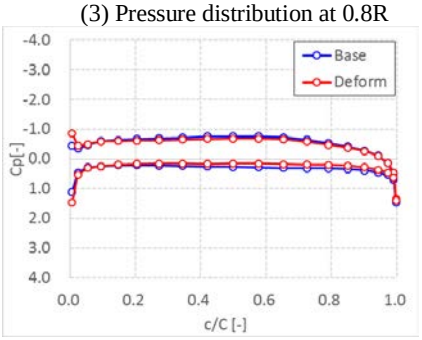

(4) Pressure distribution at 0.7R

Figure 14 Comparison propeller surface original shapes and deformed shapes at x-y plane.

5 CONCLUSIONS

In this study, the estimation method for wing shape after deformation have been developed using the image-registration. It is found that the propeller characteristics

estimated from the deformed wing shape agree well with the experimental results. From these results, it is shown that the deformation of the elastic propeller can be estimated with high accuracy by using the development method.

In the future, the authors will verify the effectiveness of the developed measurement method in non-uniform flow as the stern wake. The fluid structure interaction calculation program has been improved using these data.

ACKNOWLEGEMENT

This research was partially supported by Japan Society for the Promotion of Science (JSPS) Grant-in-Aid for Scientific Research (C) JP16K06920 and the Precise Measurement Technology Promotion Foundation (PMTP-F).

REFERENCES

Arun K. S., T. S. Huang and Blostein S. D. (1987). 'Least-Squares Fitting of Two 3-D Point Sets', IEEE Transactions on Pattern Analysis and Machine Intelligence, Vol. PAMI-9, Issue 5, pp.698-pp.700.

Hoshino, K. and Tamura, K. (2004), 'Development of Three-Dimensional Shape Measurement Method of the Object in Water', OCEANS '04. MTTS/IEEE TECHNO-OCEAN '04, Vol.3, pp.1240-1247.

Hoshino, T. (1985). 'Application of Quasi-Continuous Method to Unsteady Propeller Lifting-Surface Problems', Journal of the Society of Naval Architects of Japan, Vol. 158, pp 48-68.

Kawakita C., Takano S. and Kubo Y. (2016). 'Experimental Study on Hydrodynamic Performance of the Flexible Composite Marine Propeller', Conference Proceedings of The Japan Society of Naval Architects and Ocean Engineers, Vol.22, pp. 277-280.

Kurobe Y., Ukon Y., Koyama K. and Makino M. (1983). ' Measurement of Cavity Volume and Pressure Fluctuations on a Model of the Training Ship "SEIUN-MARU" with Reference to Full Scale Measurement', Papers of Ship Research Institute, Vol. 20, No.6, pp395-429.

Lan, C.E. (1974). 'A Quasi-Vortex-Lattice Method in Thin Wing Theory'. Journal of Aircraft, Vol.11, No.9, pp. 518-527.

Luca S., Michele V., Francesco C. and Marco F. (2009a), 'Application of computer vision techniques to measure cavitation bubble volume and cavitating tip vortex diameter', Proceedings of the 7th International Symposium on Cavitation (CAV2009), pp. 737-748.

Luca S., Michele V. and Marco F. (2009b), 'Propeller Cavitation 3D Reconstruction through Stereo-Vision Algorithms', International Conference Advanced Model Measurement Technology for EU Maritime Industry (AMT'09), pp.116-131.

Nakamura, N (1985). 'Estimation of Propeller Open-Water Characteristics Based on Quasi-Continuous Method', Journal of the Society of Naval Architects of Japan, Vol. 157, pp 95-107.

Shiraishi K., Kamiirisa H. and Koyama K. (2015), 'A Calculation Method Based on QCM for Characteristics of Propeller with Energy Saving Duct in Steady Ship's Wake', Proceedings of 4th Symposium on Marine Propulsors, pp.367-375.

Shiraishi K., Sawada Y. and Hoshino K. (2017), 'Cavity Shape Measurement Using Combination-Line CCD Camera Measurement Method', Proceedings of 5th Symposium on Marine Propulsors, pp.457-481.

Taketani T. Kimura K. Ando S and Yamamoto K. (2013). 'Study on Performance of a Ship Propeller Using a Composite Material', Proceedings of 3rd International Symposium on Marine Propulsors, pp.536-541.